

Unsteady two-temperature heat transport in mass-in-mass chains

Sergei D. Liazhkov^{1,2} and Vitaly A. Kuzkin^{2,1}

¹*Peter the Great Saint Petersburg Polytechnical University, Saint Petersburg, Russia*

²*Institute for Problems in Mechanical Engineering RAS, Saint Petersburg, Russia*

 (Received 8 February 2022; revised 30 March 2022; accepted 28 April 2022; published 25 May 2022)

We investigate the unsteady heat (energy) transport in an infinite mass-in-mass chain with a given initial temperature profile. The chain consists of two sublattices: the β -Fermi-Pasta-Ulam-Tsingou (FPUT) chain and oscillators (of a different mass) connected to each FPUT particle. Initial conditions are such that initial kinetic temperatures of the FPUT particles and the oscillators are equal. Using the harmonic theory, we analytically describe evolution of these two temperatures in the ballistic regime. In particular, we derive a closed-form fundamental solution and solution for a sinusoidal initial temperature profile in the case when the oscillators are significantly lighter than the FPUT particles. The harmonic theory predicts that during the heat transfer the temperatures of sublattices are significantly different, while initially and finally (at large times) they are equal. This may look like an artifact of the harmonic approximation, but we show that it is not the case. Two distinct temperatures are also observed in the anharmonic case, even when the heat transport regime is no longer quasiballistic. We show that the value of the nonlinearity coefficient required to equalize the temperatures strongly depends on the particle mass ratio. If the oscillators are much lighter than the FPUT particles, then a fairly strong nonlinearity is required for the equalization.

DOI: [10.1103/PhysRevE.105.054145](https://doi.org/10.1103/PhysRevE.105.054145)

I. INTRODUCTION

Far from thermal equilibrium, the concept of temperature as a single scalar parameter, characterising local thermal state of a system, may be insufficient. Therefore, in many physical problems several temperatures are introduced [1–16]. For example, molecular dynamics simulations show that the kinetic energies of thermal motion along and across the shock-wave front are different [3–6]. Temperatures, corresponding to the translational and rotational degrees of freedom in gases, also may be different [7]. In systems subjected to fast laser excitation, the temperatures of the lattice and electronic subsystem are different [8–13]. Many other examples of several-temperature systems are given in review Refs. [14–16]. In the present paper, we focus on yet another example of nonequilibrium system with several distinct temperatures, namely a heat conducting anharmonic chain.

In heat conducting lattices, several temperatures are observed, for instance, in the nonequilibrium steady state (NESS). This state is realized in the systems placed between two thermostats with different temperatures (see, e.g., Ref. [17]). In the NESS, kinetic temperatures of sublattices may be different in both harmonic [18,19] and anharmonic [20] crystals. For example, in Ref. [18] it is shown that kinetic temperatures of the two sublattices of the chain with alternating masses are different. In Ref. [20] the several distinct temperatures are observed in the diatomic β -FPUT chain near the thermostats. These studies show that in systems under continuous external excitation the kinetic temperatures may be different.

After external excitation, the kinetic temperatures usually tend to a single equilibrium value. This process is investigated, for example, in uniformly heated triangle [21] and

face-centered cubic [22] lattices with Lennard-Jones interactions. In these lattices, initial nonequilibrium state was created by specifying random velocities of atoms in one direction. Then initial kinetic temperatures corresponding to different spatial directions are distinct. It is shown that equilibration of the temperatures during transition to thermal equilibrium requires some time. In the case of weak anharmonicity (e.g., at low temperatures), this time is inversely proportional to the initial kinetic temperature [22]. Therefore, equilibration of kinetic temperatures may take a long time.

To the best of our knowledge, papers on unsteady heat transport in chains with several kinetic temperatures are scarce. Analytical description of unsteady heat transport in harmonic approximation is presented in Ref. [23]. It is shown that in heat conducting harmonic crystals temperatures, corresponding to degrees of freedom of the unit cell, may be different even if initially they are equal. Then questions arise of whether similar effect may be observed in anharmonic crystals and what degree of nonlinearity is required for equalization of the temperatures.

To address these important questions quantitatively, we study unsteady heat transport in the mass-in-mass chain, consisting of the β -FPUT chain and oscillators (of different mass) attached to each FPUT particle. In the harmonic case, we present an analytical solution describing evolution of the two-temperature fields, corresponding to FPUT chain and oscillators. In the anharmonic case, there is a “competition” between two processes, having different characteristic timescales: heat transport and equalization of the two temperatures. For weak anharmonicity, decay of thermal perturbation, caused by heat transport, is significantly faster than the equalization of temperatures. Then the temperatures

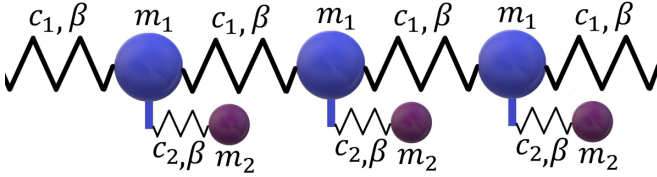


FIG. 1. The mass-in-mass chain, consisting of the β -FPUT chain and additional nonlinear oscillators.

remain different during the heat transport. The rate of equalization increases with increasing nonlinearity. Therefore, the temperatures equalize before the decay of thermal perturbation provided that the nonlinearity is sufficiently strong. We also show that the key parameter, determining the results of this competition, is the ratio of particle masses.

II. STATEMENT OF THE PROBLEM

A. Equations of motion and initial conditions

We consider unsteady heat transport in a diatomic chain consisting of the β -Fermi-Pasta-Ulam-Tsingou (FPUT)¹ chain and nonlinear oscillators, connected to each FPUT particle (see Fig. 1). The FPUT particles have mass m_1 , while the oscillators have mass m_2 . For $\beta = 0$, this model is usually referred to as the mass-in-mass chain. It is extensively studied as the simplest model of an acoustic metamaterial [24–34]. It may also be considered as a model for hydrocarbon chains. To the best of our knowledge, unsteady heat transport in the mass-in-mass chain has not been studied systematically. Dynamics equations for the unit cell j have the form

$$\begin{aligned} m_1 \ddot{u}_{1,j} &= c_1(u_{1,j+1} - 2u_{1,j} + u_{1,j-1}) + c_2(u_{2,j} - u_{1,j}) \\ &\quad + \beta(u_{2,j} - u_{1,j})^3 + \beta[(u_{1,j+1} - u_{1,j})^3 \\ &\quad + (u_{1,j-1} - u_{1,j})^3], \\ m_2 \ddot{u}_{2,j} &= c_2(u_{1,j} - u_{2,j}) + \beta(u_{1,j} - u_{2,j})^3, \end{aligned} \quad (1)$$

where $u_{1,j}$ and $u_{2,j}$ are displacements of the FPUT particles and attached oscillators; c_1 is the stiffness of the FPUT chain; c_2 is the stiffness of the oscillators; $\beta \geq 0$ is a parameter characterizing anharmonicity. In further calculations, we take $c_1 = c_2 = c$. Equations (1) are supplemented by the periodic boundary conditions.

We consider evolution of the initial temperature profile in an isolated chain. The initial temperature profile is created by specifying random initial velocities of the particles [36]:

$$\begin{aligned} u_{1,j} &= u_{2,j} = 0, \\ \dot{u}_{1,j} &= \rho_{1,j} \sqrt{k_B T_j^0 / m_1}, \quad \dot{u}_{2,j} = \rho_{2,j} \sqrt{k_B T_j^0 / m_2}, \end{aligned} \quad (2)$$

where k_B is the Boltzmann constant; T_j^0 is the initial temperature of particles from the unit cell j [see definition

¹Since we study heat transport only, we consider thermal expansion negligible. Interactions by the β -FPUT potential [in contrast to α -FPUT (see, e.g., Ref. [35])] exclude the latter, allowing not to separate thermal and mechanical motions. For these reasons, we formulate the problem.

Eq. (5)]; $\rho_{1,j}, \rho_{2,j}$ are uncorrelated random values with zero mathematical expectation and unit variance, i.e., $\langle \rho_{1,j} \rangle = \langle \rho_{2,j} \rangle = 0$, $\langle \rho_{1,j} \rho_{2,j} \rangle = 0$, $\langle \rho_{1,j}^2 \rangle = \langle \rho_{2,j}^2 \rangle = 1$. Note that initial conditions Eq. (2) are such that for each unit cell initial temperatures of the FPUT particle and the oscillator are equal.

B. Temperatures of sublattices

To define the kinetic temperature, we consider an infinite set of realizations of system Eq. (1) with random initial conditions Eq. (2). It is shown below that during the heat transport, kinetic temperatures of the FPUT particles and oscillators are generally different. Therefore, we introduce the temperature matrix T [23]:

$$k_B T_j = \begin{pmatrix} m_1 \langle \dot{u}_{1,j}^2 \rangle & \sqrt{m_1 m_2} \langle \dot{u}_{1,j} \dot{u}_{2,j} \rangle \\ \sqrt{m_1 m_2} \langle \dot{u}_{2,j} \dot{u}_{1,j} \rangle & m_2 \langle \dot{u}_{2,j}^2 \rangle \end{pmatrix}. \quad (3)$$

The diagonal elements of T determine kinetic temperatures of sublattices, i.e., temperatures of the FPUT particles and oscillators, respectively,

$$k_B T_{11,j} = m_1 \langle \dot{u}_{1,j}^2 \rangle, \quad k_B T_{22,j} = m_2 \langle \dot{u}_{2,j}^2 \rangle. \quad (4)$$

The off-diagonal components of the temperature matrix characterize correlations between particle velocities. We also introduce a conventional (average) kinetic temperature, defined as

$$T_j = \frac{1}{2}(T_{11,j} + T_{22,j}). \quad (5)$$

Therefore, initial conditions Eq. (2) imply some initial temperature profile and *equal* kinetic temperatures of the sublattices. Time evolution of the temperatures $T_{11,j}$ and $T_{22,j}$ is considered below.

III. HEAT TRANSPORT IN HARMONIC CASE

In the absence of anharmonicity ($\beta = 0$), the thermal energy is carried by noninteracting waves (or wave packets [37]), propagating freely through the chain. This regime of heat transport is usually referred to as the ballistic heat transport. In this section, we present an analytical solution, describing ballistic heat transport in the harmonic MiM chain. We show that during the heat transport the kinetic temperatures $T_{11,j}$ and $T_{22,j}$, corresponding to the FPUT particles and oscillators, are essentially different even though initially and finally (at large times) they are equal.

A. Dispersion relation and group velocities

To analyze heat transport in the harmonic crystals, the dispersion relation is required (see, e.g., Refs. [23,36,38,39]). We rewrite Eqs. (1) and (2) for $\beta = 0$ in a matrix form:

$$\begin{aligned} M \ddot{\mathbf{u}}_j &= C_1 \mathbf{u}_{j+1} + C_0 \mathbf{u}_j + C_{-1} \mathbf{u}_{j-1}, \\ M &= \begin{pmatrix} m_1 & 0 \\ 0 & m_2 \end{pmatrix}, \quad C_1 = C_{-1} = c \begin{pmatrix} 1 & 0 \\ 0 & 0 \end{pmatrix}, \\ C_0 &= c \begin{pmatrix} -3 & 1 \\ 1 & -1 \end{pmatrix}, \quad \mathbf{u}_j = [u_{1,j} \quad u_{2,j}]^\top, \end{aligned} \quad (6)$$

where \top stands for the transpose sign; matrices $C_{\pm 1}$ define stiffness of springs, connecting the cell j with the neighboring

cell, and the matrix \mathbf{C}_0 describes interaction of particles inside the cell j .

To obtain a dispersion relation, $\omega(k)$, we seek the solution of Eq. (6) in the form

$$\mathbf{u}_j = \mathbf{U} e^{i(\omega t + k j)}, \quad t^2 = -1, \quad (7)$$

where $k \in [0; 2\pi]$ is the wave number and \mathbf{U} is a constant vector. Substituting Eq. (7) into Eq. (6) yields the homogeneous system of linear equations with respect to \mathbf{U} :

$$\begin{aligned} (\mathbf{\Omega} - \omega^2 \mathbf{I})\mathbf{U} &= 0, \\ \mathbf{\Omega} &= -\mathbf{M}^{-\frac{1}{2}} \mathbf{C}_0 \mathbf{M}^{-\frac{1}{2}} - 2\mathbf{M}^{-\frac{1}{2}} \mathbf{C}_1 \mathbf{M}^{-\frac{1}{2}} \cos k, \end{aligned} \quad (8)$$

where $\mathbf{\Omega}$ is the dynamical matrix of the chain; \mathbf{I} is the 2×2 identity matrix. The matrix $\mathbf{\Omega}$ is real and symmetric and therefore, it is represented as

$$\mathbf{\Omega} = \mathbf{P} \mathbf{\Lambda} \mathbf{P}^\top, \quad \mathbf{\Lambda} = \begin{pmatrix} \omega_1^2 & 0 \\ 0 & \omega_2^2 \end{pmatrix}, \quad (9)$$

where $\mathbf{P}(k)$ is an orthogonal matrix, composed of unit eigenvectors of $\mathbf{\Omega}$; $\omega_{1,2}(k)$ are acoustic and optical branches of the dispersion relation, respectively,

$$\begin{aligned} \omega_{1,2}(k) &= \frac{\omega_e}{\sqrt{\gamma}} \sqrt{R(k) \mp \sqrt{R^2(k) - 4\gamma \sin^2 \frac{k}{2}}}, \\ R(k) &= \frac{1+\gamma}{2} + 2\gamma \sin^2 \frac{k}{2}, \quad \omega_e = \sqrt{\frac{c}{m_1}}, \quad \gamma = \frac{m_2}{m_1}. \end{aligned} \quad (10)$$

Here the minus sign corresponds to the acoustic branch of the dispersion relation, ω_1 , while the plus sign corresponds to the optical branch ω_2 .

One of the key parameters of the problem is the mass ratio $\gamma = m_2/m_1$. The dispersion relation for different values of γ is shown in Fig. 2(a). The parameter controls, in particular, the bandgap $\delta\omega$, defined as the difference between maximum acoustic frequency and minimum optical frequency:

$$\begin{aligned} \delta\omega &= \min \omega_2 - \max \omega_1 \\ &= \frac{\omega_e}{\sqrt{2\gamma}} \left(\sqrt{2(1+\gamma)} - \sqrt{1+5\gamma - \sqrt{1+\gamma(25\gamma-6)}} \right). \end{aligned} \quad (11)$$

Equation (11) shows that the bandgap tends to infinity as γ tends to zero and it tends to the cutoff frequency of harmonic chain on a linear elastic foundation as γ tends to infinity. Unsteady thermal processes in this system are studied, e.g., in

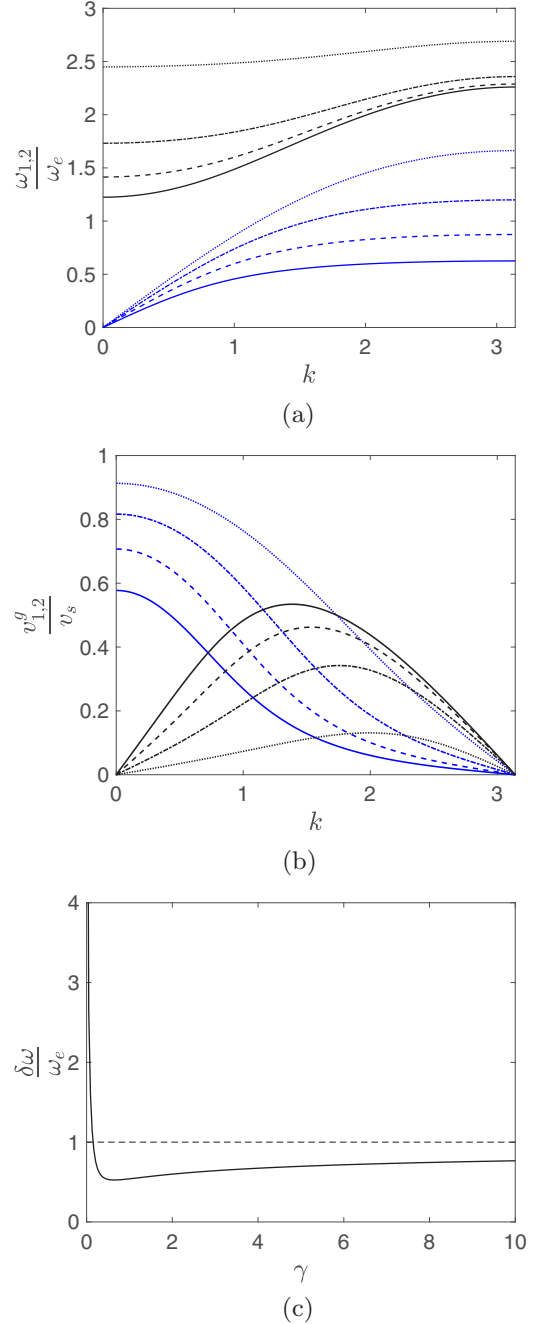


FIG. 2. Acoustic (blue lines) and optical (black lines) branches of the dispersion relation (a) and corresponding group velocities (b) for different mass ratios: $\gamma = 2$ (solid line), $\gamma = 1$ (dashed line), $\gamma = \frac{1}{2}$ (dash-dotted line), and $\gamma = \frac{1}{5}$ (dotted line). The bandgap as a function of the mass ratio γ (c).

Refs. [41,42]. Dependence of the bandgap on the mass ratio γ is shown in Fig. 2(c). The figure shows, in particular, that the dependence is nonmonotonic. The bandgap has minimal value at $\gamma_* \approx 0.646$.

The mass ratio also significantly influences the group velocities, which determine the shape and speed of thermal waves in the ballistic regime (see, e.g., Refs. [23,38,39]). The

group velocities are calculated as

$$v_{1,2}^g(k) \stackrel{\text{def}}{=} a \frac{d\omega_{1,2}}{dk},$$

$$v_{1,2}^g = \frac{v_s \sqrt{\gamma}}{2} \frac{\left(1 \pm \frac{1-R(k)}{\sqrt{R^2(k)-4\gamma \sin^2 \frac{k}{2}}}\right) \sin k}{\sqrt{R(k) \mp \sqrt{R^2(k)-4\gamma \sin^2 \frac{k}{2}}}},$$

$$v_s = \omega_e a, \quad (12)$$

where v_s is the sound speed.

If the oscillators are significantly lighter than the FPUT particles ($\gamma \ll 1$), then we have the following series expansions of acoustic and optical group velocities:

$$v_1^g = v_s \left(1 - \frac{\gamma}{2}\right) \cos \frac{k}{2} + O(\gamma^2),$$

$$v_2^g = v_s \gamma^{\frac{3}{2}} \sin k + O(\gamma^{\frac{5}{2}}). \quad (13)$$

Equation (13) shows that for small γ the optical group velocities are significantly smaller than the acoustic ones. This fact is clearly seen in Fig. 2(b). We show below that this difference between group velocities strongly affects the heat transfer. Equation (13) allows to derive approximate closed-form solutions of heat transfer problems (see Sec. III D 4).

B. The general solution of the ballistic heat transfer problem

The general solution, describing evolution of the kinetic temperature Eq. (5) in continuum approximation, has the form (see Ref. [23] for derivation):

$$T(x, t) = T^F(x, t) + T^S(x, t),$$

$$T^F(x, t) = \frac{T^0(x)}{8\pi} \sum_{j=1}^2 \int_0^{2\pi} \cos(2\omega_j(k)t) dk,$$

$$T^S(x, t) = \frac{1}{8\pi} \sum_{j=1}^2 \int_0^{2\pi} T^0(x + v_j^g(k)t) dk, \quad (14)$$

where x is a continuous spatial coordinate. Here and below the continuous temperature field $T(x, t)$ is considered. It is assumed that the temperature T_j of the unit cell j coincides with $T(aj, t)$; $T^0(x)$ is the initial temperature profile. The term T^F corresponds to the high frequency of oscillations of the kinetic temperatures, caused by equilibration of kinetic and potential energies.² This process is considered in details, e.g., in Refs. [21,22,38,43,44]. The term T^S describes slow changes of the kinetic temperature profile caused by ballistic heat transport. Each of the terms T^F , T^S is equal to a sum of contributions of acoustic and optical branches of the dispersion relation.

²The initial conditions Eq. (2) are such that the total energy of the chain is equal to its initial kinetic energy, while the potential energy is equal to zero. Motion of the particles leads to partial conversion of energy from kinetic to potential form (in the harmonic case the energies become equal). This fast process is described by the term T^F in Eq. (14).

We note that the solution Eq. (14) is derived in Ref. [23] via continualization of the exact expression for the temperature field, which in turn is obtained using the solution of lattice dynamics equations. During the derivation, no concrete relations between the temperature and the heat flux were used. To the best of our knowledge, in the unsteady ballistic case these relations are known only for some particular cases (see, e.g., Ref. [36]). Therefore, we further focus on the behavior of the temperature field. Discussion of the corresponding heat fluxes is beyond the scope of the present paper.

In the following subsection, we employ the Eq. (14) for analysis of evolution of a point temperature perturbation.

C. Fundamental solution

Since the ballistic heat transport problem is linear, the evolution of any initial temperature field is completely determined by the fundamental solution. To obtain the fundamental solution we consider

$$T^0(x) = \mathcal{A} \delta(x), \quad (15)$$

where $\delta(x)$ is a Dirac δ function; \mathcal{A} is a constant of $\text{K} \cdot \text{m}$ dimension. Substituting Eq. (15) into Eq. (14) and neglecting T^F , we obtain

$$T \approx T^S = T_{\text{ac}} + T_{\text{op}},$$

$$T_{\text{ac}} = \frac{\mathcal{A}}{8\pi} \int_0^{2\pi} \delta(x + v_1^g(k)t) dk,$$

$$T_{\text{op}} = \frac{\mathcal{A}}{8\pi} \int_0^{2\pi} \delta(x + v_2^g(k)t) dk, \quad (16)$$

where T_{ac} and T_{op} determine contributions of acoustic and optical branches of the dispersion relation, respectively.

Calculation of integrals in Eq. (16) is carried out using the following equation [45]:

$$\int_{\mathcal{D}} \delta(f(\xi)) d\xi = \sum_j |f'(\xi_j)|^{-1}, \quad f(\xi_j) = 0, \quad (17)$$

where ξ_j are zeros of function f , lying inside the domain \mathcal{D} . The calculation yields the following expressions for contributions T_{ac} and T_{op} :

$$T_{\text{ac}} = \frac{\mathcal{A}}{8\pi t} \sum_j \left| \frac{dv_1^g}{dk} \Big|_{k=k_j} \right|^{-1}, \quad v_1^g(k_j) = \frac{|x|}{t},$$

$$T_{\text{op}} = \frac{\mathcal{A}}{8\pi t} \sum_j \left| \frac{dv_2^g}{dk} \Big|_{k=k_j} \right|^{-1}, \quad v_2^g(k_j) = \frac{|x|}{t}. \quad (18)$$

Here summation is carried out with respect to roots of equations $v_j^g(k) = |x|/t$. From Eqs. (12) and (18) it is seen that functions T_{ac} and T_{op} are even with respect to zero. The fundamental solution multiplied by t depends on the self-similar variable x/t .

For $\gamma \ll 1$ the fundamental solution Eq. (18) is represented in the closed form. Substituting the approximate expressions Eq. (13) for the group velocities into Eq. (18), we

obtain

$$\begin{aligned} T_{ac} &\approx \frac{\mathcal{A}H(w_1t - |x|)}{4\pi\sqrt{w_1^2t^2 - x^2}}, & w_1 &= \max v_1^g, \\ T_{op} &\approx \frac{\mathcal{A}H(w_2t - |x|)}{4\pi\sqrt{w_2^2t^2 - x^2}}, & w_2 &= \max v_2^g, \end{aligned} \quad (19)$$

where $H(x)$ is the Heaviside function and w_1, w_2 are maximum group velocities. Equation (19) shows that for small γ contributions of acoustic and optical branches have the same form as the fundamental solution for the Hooke chain, obtained in Ref. [36]. Our calculations show that the Eq. (19) has reasonable accuracy approximately for $\gamma \leq 0.05$.

Contributions of acoustic and optical branches of dispersion relation to the fundamental solution for different mass ratios γ are shown in Fig. 3.

We note that areas under the curves, corresponding to contributions of acoustic and optical branches, are equal. Therefore, the total amount of energy carried by acoustic and optical waves is the same. It is seen from Fig. 3 that for $\gamma \ll 1$, optical front propagates significantly slower than the acoustic front, because $v_2^g \ll v_s$. For $\gamma = 2$, optical and acoustic fronts propagate synchronously, since the corresponding maximum group velocities are equal.

We also note that, for $\gamma = 1/2, 1, 2$, the acoustic part of the fundamental solution has a local maximum at $x = 0$. This fact may be explained in terms of the kinetic theory. In the framework of this theory the heat is carried by quasiparticles (wave packets) moving with the group velocities. Physical meaning of these quasiparticles is discussed, e.g., in Ref. [37]. For large values of γ , the number of the acoustic quasiparticles with small group velocities is relatively large [see Fig. 2(b)]. Therefore, these slow quasiparticles form the local maximum at $x = 0$. The relative number of the slow quasiparticles decreases with increasing γ . Therefore, for $\gamma < 0.1027$ the local maximum vanishes.

Thus the fundamental solution strongly depends on the mass ratio γ . For small γ , it is represented in the closed form Eq. (19). Further, we show that γ also influences the behavior of temperatures of sublattices T_{11}, T_{22} in both harmonic and anharmonic cases. We mostly focus on the two cases $\gamma = 2$ (heavy oscillators) and $\gamma = 1/10$ (light oscillators), corresponding to significantly different fundamental solutions (see Fig. 3).

D. Sinusoidal initial temperature profile. Two temperatures

In this subsection, we study the decay of the sinusoidal temperature profiles at different mass ratios γ . The main goal is to describe analytically the behavior of temperatures T_{11}, T_{22} , defined by Eq. (4). In particular, we show that during heat transfer the temperatures are significantly different while initially and finally (at $t \rightarrow \infty$) they are equal.

1. Analytical solution

We consider the following initial temperature profile:

$$T^0(x) = T_b + \Delta T \sin \frac{2\pi x}{L}, \quad (20)$$

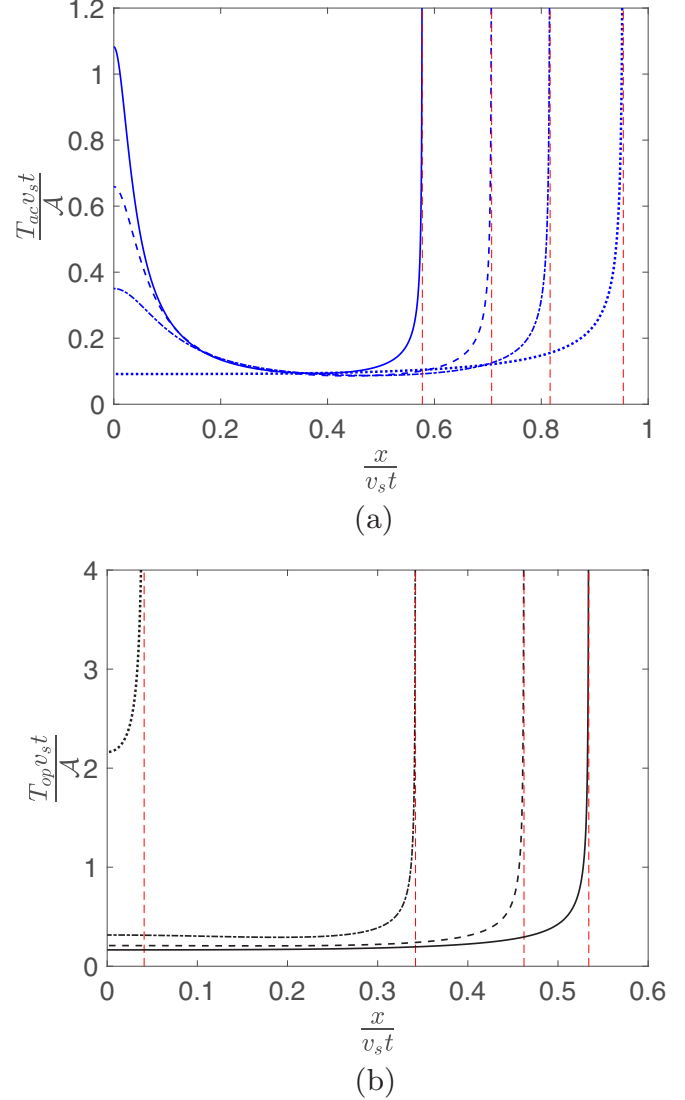


FIG. 3. Contributions of acoustic (a) and optical (b) branches of dispersion relation to the fundamental solution [Eq. (18)] for $\gamma = 2$ (solid line), 1 (dashed line), 1/2 (dash dotted line), and 1/10 (dotted line). Vertical asymptotes at $x = t \max v_j^g$ (red dashed lines) are also shown.

where T_b is the background temperature; ΔT is the amplitude of sine; L is the length of the periodic cell. The initial temperatures of sublattices are equal, i.e., $T_{11} = T_{22} = T^0$. This profile is chosen because it can be realized in real experiments based on the transient thermal grating technique (see, e.g., Refs. [46,47]).

The evolution of the temperature matrix \mathbf{T} , defined by Eq. (3), is described as

$$\begin{aligned} \mathbf{T}(x, t) &= \mathbf{T}^F(x, t) + \mathbf{T}^S(x, t), \\ \mathbf{T}^F(x, t) &= \frac{1}{2} \left(T_b + \Delta T \sin \frac{2\pi x}{L} \right) \mathbf{F}(t), \\ \mathbf{T}^S(x, t) &= \frac{1}{2} \left[T_b \mathbf{I} + \Delta T \mathbf{S}(t) \sin \frac{2\pi x}{L} \right], \end{aligned} \quad (21)$$

where

$$\mathbf{F}(t) = \frac{1}{2\pi} \int_0^{2\pi} \mathbf{P} \tilde{\mathbf{F}} \mathbf{P}^\top dk, \quad \mathbf{S}(t) = \frac{1}{2\pi} \int_0^{2\pi} \mathbf{P} \tilde{\mathbf{S}} \mathbf{P}^\top dk,$$

$$\tilde{F}_{ij} = \delta_{ij} \cos(2\omega_j t), \quad \tilde{S}_{ij} = \delta_{ij} \cos \frac{2\pi v_j^s t}{L}, \quad (22)$$

and δ_{ij} is the Kronecker delta. Detailed derivation of Eq. (21) for different lattices is given in Ref. [23]. Here $\mathbf{F}(t)$ describes changes of temperatures due to equilibration of kinetic and potential energies [for details see the explanation after Eq. (14)], while $\mathbf{S}(t)$ describes the changes due to ballistic heat transport. These two physical processes have significantly different timescales. At short times, of order of 100 periods of atomic vibrations, $\mathbf{F}(t)$ oscillates in time and tends to zero. At larger times, changes in amplitude caused by ballistic heat transfer are described by $\mathbf{S}(t)$. The characteristic timescale of this process is of order of $|L/v_j^s|$. In further analysis we consider large time behavior of the temperature and therefore $\mathbf{F}(t)$ is neglected. Then the temperatures of sublattices are equal to

$$T_{11}(x, t) = \frac{1}{2} \left[T_b + \Delta T S_{11}(t) \sin \frac{2\pi x}{L} \right],$$

$$T_{22}(x, t) = \frac{1}{2} \left[T_b + \Delta T S_{22}(t) \sin \frac{2\pi x}{L} \right], \quad (23)$$

where S_{jj} are diagonal elements of the matrix \mathbf{S} .

According to Eq. (23), the temperature profiles remain sinusoidal for any moment in time. At $t \rightarrow \infty$, the functions S_{jj} tend to zero. Therefore, finally the temperatures T_{11} and T_{22} become equal even though the system is harmonic. Spatially averaged values of the temperatures are also equal to each other. Further, we focus on evolution of the amplitudes of temperature profiles defined as

$$A_{jj}(t) = \frac{2}{L} \int_0^L T_{jj}(x, t) \sin \frac{2\pi x}{L} dx. \quad (24)$$

We show below that during the heat transfer the amplitudes are generally different.

Analytical expressions for the amplitudes are obtained by substituting Eq. (23) into Eq. (24):

$$A_{jj} = \Delta T S_{jj}/2. \quad (25)$$

Comparison of the analytical solution Eq. (25) with results of numerical simulations is presented below. We also investigate contributions of acoustic and optical vibrations to the amplitudes A_{jj} . According to the definition Eq. (22) of \mathbf{S} , the contributions have the following form:

$$A_{jj} = A_{jj}^{\text{ac}} + A_{jj}^{\text{op}}, \quad A_{jj}^{\text{ac}} = \frac{\Delta T}{4\pi} \int_0^{2\pi} P_{j1}^2 \cos \frac{2\pi v_1^s t}{L} dk,$$

$$A_{jj}^{\text{op}} = \frac{\Delta T}{4\pi} \int_0^{2\pi} P_{j2}^2 \cos \frac{2\pi v_2^s t}{L} dk. \quad (26)$$

Closed-form expressions for A_{11} and A_{22} in terms of Bessel functions for small γ (light oscillators) are derived below [see Eq. (31)].

2. Simulation details

In numerical simulations, we integrate equations of motion Eq. (1) by the fourth-order symplectic method [50,51], with initial conditions³ Eqs. (2) and (20) and periodic boundary conditions. The amplitudes of temperatures of sublattices A_{11} and A_{22} are calculated by Eq. (24). Integrals in these formulas are replaced by sums over all particles in the periodic cell. Temperatures are calculated by the definition Eq. (4), where the mathematical expectation is replaced by averaging over N_r realizations. The following values of parameters are used:

$$N = 10^3, \quad N_r = 10^4, \quad \Delta T = 0.1T_b,$$

$$\Delta t = 2 \times 10^{-3} \tau_e, \quad \tau_e = 2\pi/\omega_e, \quad \beta = 0, \quad (27)$$

where N is the number of particles, Δt is the time step, and ω_e is defined by Eq. (10).

3. Heavy oscillators ($\gamma = 2$)

In this subsection, we compare the analytical Eq. (26) for amplitudes A_{11}, A_{22} of temperatures T_{11}, T_{22} with results of numerical simulations. We also analyze contributions of acoustic and optical vibrations to behavior of the temperatures. The mass ratio $\gamma = 2$ is considered. In this case, the maximum acoustic and optical group velocities are of the same order.

The behavior of amplitudes of the temperatures is shown in Fig. 4. It is seen that numerical and analytical solutions practically coincide with each other. The figure shows that during the heat transfer the temperatures T_{11} and T_{22} are different. Both amplitudes perform decaying oscillations. Such behavior is typical for systems with ballistic heat transport (see, e.g., Refs. [23,36,38,52]). It is also seen that periods of temperature oscillations are of the same order. This is due to the fact that acoustic and optical group velocities are close.

At large times, the main contribution to A_{11} (temperature of FPUT particles) is given by acoustic vibrations, while the main contribution to A_{22} (temperature of oscillators) is given by optical vibrations. Our calculations show that for other values of $\gamma = O(1)$ similar behavior is observed.

4. Light oscillators ($\gamma \ll 1$): Ballistic spectra inversion

In this subsection, we derive an approximate closed-form solutions for the amplitudes A_{11}, A_{22} of temperatures for the case when oscillators are significantly lighter than the FPUT particles ($\gamma \ll 1$). We also show that low-frequency (acoustic) oscillations of atoms cause high-frequency oscillations of temperature and vice versa. This new phenomenon, introduced in the present paper, is further referred to as the ‘‘ballistic spectra inversion.’’

For example, we consider the case $\gamma = 1/10$. Time evolution of the amplitudes A_{11} and A_{22} obtained analytically and numerically is shown in Fig. 5. As in the previous case ($\gamma = 2$), the amplitudes perform decaying oscillations. However, in contrast to the previous case, the oscillations have two significantly different main frequencies. It is also seen that the main contribution to the temperature of the FPUT particles (A_{11}) is given by acoustic vibrations, while the main

³We take uniform distribution of the random numbers $\rho_{1,j}$ and $\rho_{2,j}$.

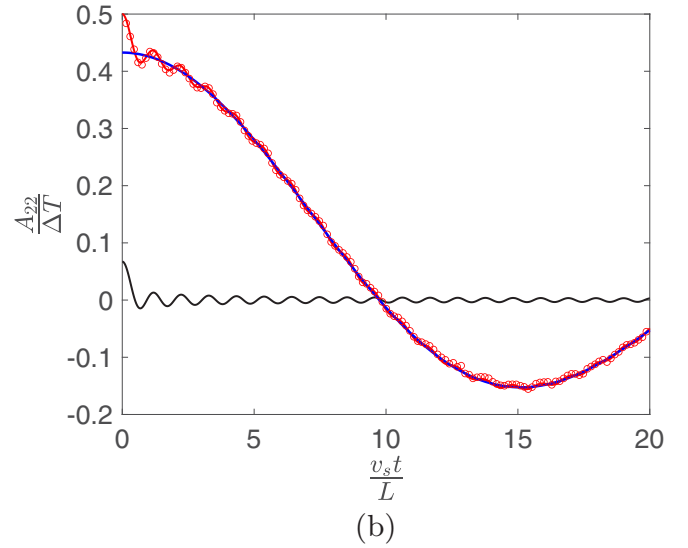
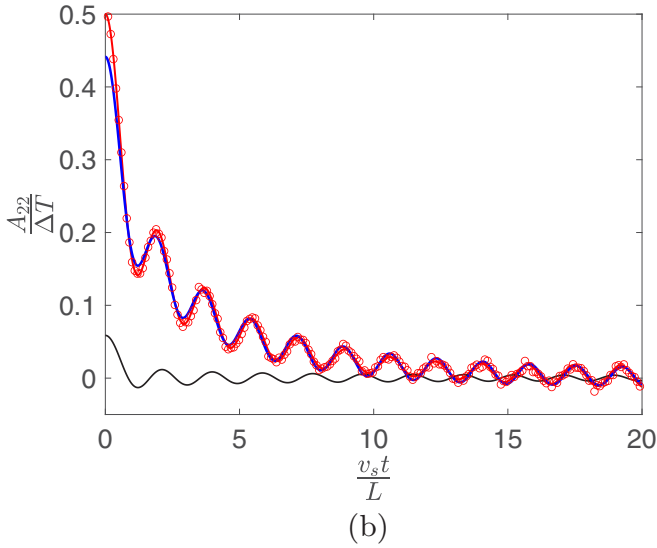
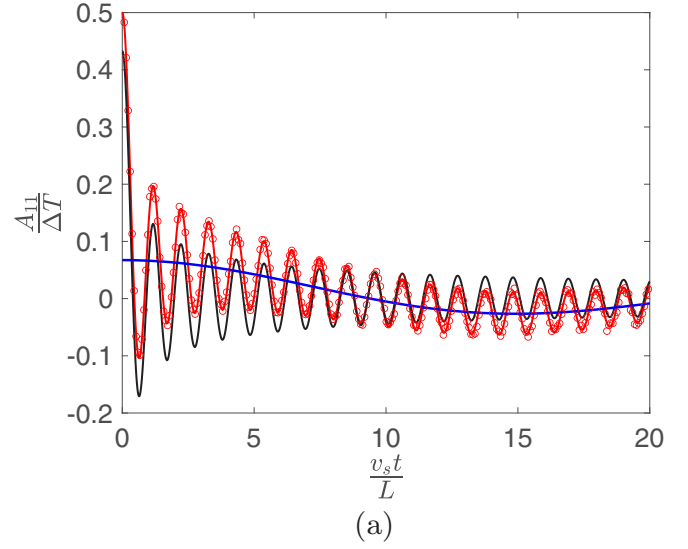
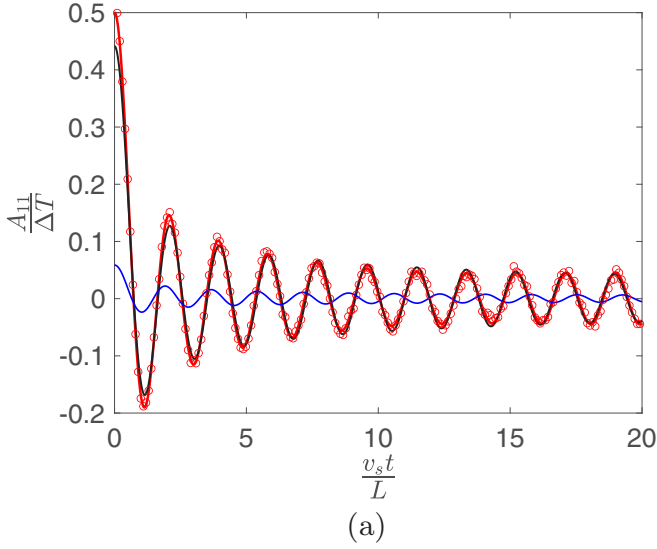


FIG. 4. Decay of the amplitudes A_{11} (a) and A_{22} (b) of the kinetic temperatures for $\gamma = 2$. Analytical (red solid line) and numerical (red circles) solutions are shown. Contributions of acoustic (black solid line) and optical (blue line) branches of dispersion relation are shown.

FIG. 5. Decay of the amplitudes A_{11} (a) and A_{22} (b) of the kinetic temperatures for $\gamma = 1/10$. Analytical (red solid line) and numerical (red circles) solutions are shown. Contributions of acoustic (black solid line) and optical (blue line) branches of dispersion relation are shown.

contribution to the temperature of the oscillators (A_{22}) is given by the optical vibrations. To explain these facts, we derive an approximate closed-form solution for A_{jj} .

The solution is derived, assuming $\gamma \ll 1$. In this case, the group velocities are approximated by Eq. (13) as

$$v_1^g \approx w_1 \cos \frac{k}{2}, \quad v_2^g \approx w_2 \sin k, \quad (28)$$

where w_1 , w_2 are maximum group velocities, defined by Eq. (19). Substitution of Eq. (28) into Eqs. (26) for A_{jj}^{ac} and A_{jj}^{op} then yields

$$\begin{aligned} A_{jj}^{\text{ac}} &\approx \frac{\Delta T}{4\pi} \int_0^{2\pi} P_{j1}^2 \cos\left(\frac{2\pi w_1 t}{L} \cos \frac{k}{2}\right) dk, \\ A_{jj}^{\text{op}} &\approx \frac{\Delta T}{4\pi} \int_0^{2\pi} P_{j2}^2 \cos\left(\frac{2\pi w_2 t}{L} \sin k\right) dk. \end{aligned} \quad (29)$$

It follows from analysis of Eq. (29) that for small γ the elements P_{ij}^2 slowly change with k . Therefore, we take the average values of P_{ij}^2 out the integral. The remaining integrals are represented in terms of the Bessel function of the first kind, J_0 , as

$$\begin{aligned} A_{11} &\approx \frac{\Delta T}{2} \left[(1 - \varepsilon) J_0\left(\frac{2\pi}{L} w_1 t\right) + \varepsilon J_0\left(\frac{2\pi}{L} w_2 t\right) \right], \\ A_{22} &\approx \frac{\Delta T}{2} \left[\varepsilon J_0\left(\frac{2\pi}{L} w_1 t\right) + (1 - \varepsilon) J_0\left(\frac{2\pi}{L} w_2 t\right) \right], \\ \varepsilon &= 1 - \frac{1}{2\pi} \int_0^{2\pi} P_{11}^2 dk \approx \gamma + 3\gamma^2. \end{aligned} \quad (30)$$

Equation (30) yields the closed form solution of the heat transport problem with sinusoidal temperature profile. Comparison of the complete analytical solution Eq. (26) with approximate

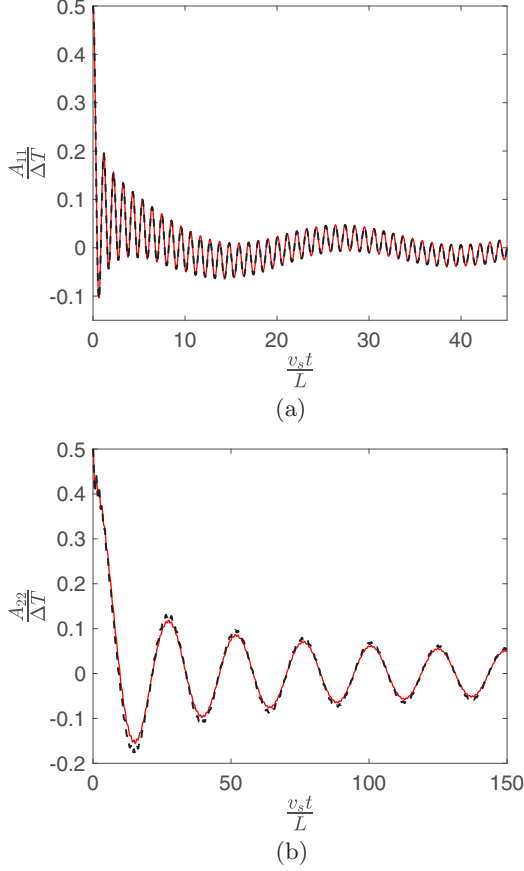


FIG. 6. The complete solution [Eq. (26), red solid line] and approximate solution [Eq. (30), black dashed line] for the amplitudes A_{11} (a) and A_{22} (b) at $\gamma = 1/10$.

Eq. (30) for $\gamma = 1/10$ is presented in Fig. 6. It is seen from Fig. 6 that approximate and complete solutions are in a good quantitative agreement.

We continue analysis of Eq. (30). It clearly shows that the solution has two characteristic frequencies, proportional to maximum acoustic and optical group velocities (w_1, w_2). For small γ these frequencies are significantly different, because $w_1 \gg w_2$. Moreover, in this case $\varepsilon \ll 1$ and therefore Eq. (30) reduces to

$$A_{11} \approx \frac{\Delta T}{2} J_0\left(\frac{2\pi}{L} w_1 t\right), \quad A_{22} \approx \frac{\Delta T}{2} J_0\left(\frac{2\pi}{L} w_2 t\right). \quad (31)$$

Equation (31) shows that the main contribution to high-frequency oscillations of A_{11} is given by the low-frequency acoustic vibrations of the chain, while low-frequency oscillations of A_{22} are due to high-frequency optical oscillations of the chain. We refer to this phenomenon as the “ballistic spectra inversion.”

In the next section, we investigate how anharmonicity affects on evolution and equalization of the temperatures of FPUT particles (A_{11}) and oscillators (A_{22}).

IV. TWO TEMPERATURES IN THE ANHARMONIC CHAIN

In this section, we study influence of anharmonic interactions on the solution of the heat transport problem with

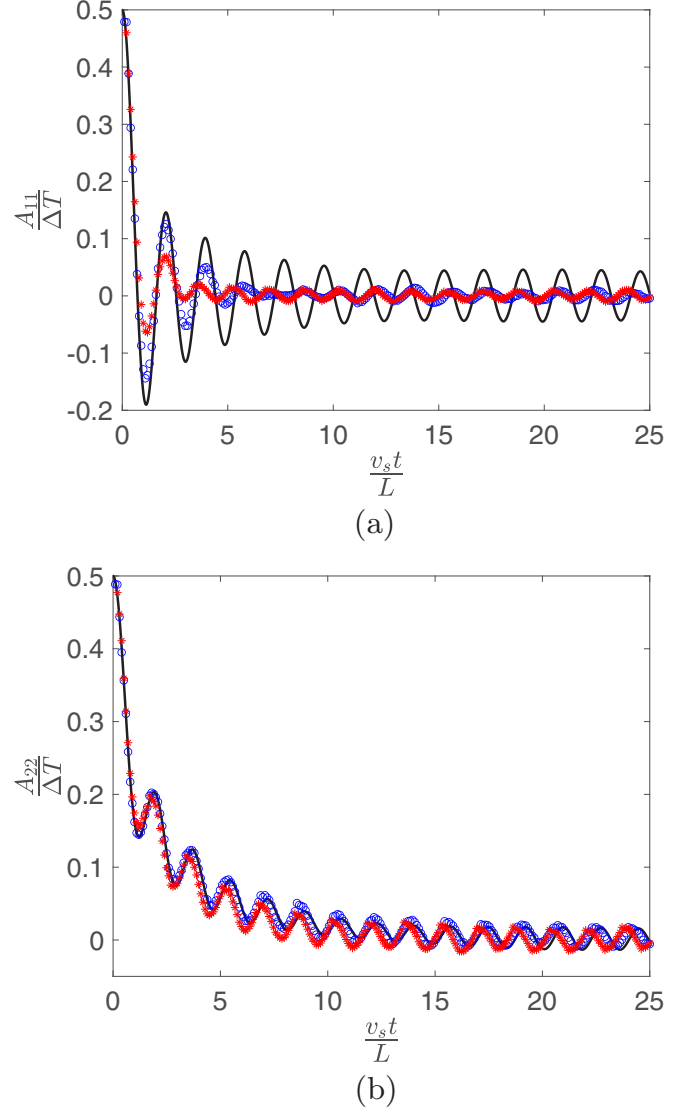


FIG. 7. The amplitudes A_{11} (a) and A_{22} (b) of sinusoidal temperature profiles in the weakly anharmonic case for $\gamma = 2$. The analytical solution [Eq. (26), solid line] and numerical simulation results for $\tilde{\beta} = 0.05$ (blue circles), $\tilde{\beta} = 0.1$ (red asterisks) are shown.

sinusoidal initial temperature profile Eq. (20). The problem is solved numerically for different values of the dimensionless parameter $\tilde{\beta}$, characterizing anharmonicity:

$$\tilde{\beta} = k_B T_b \beta / c^2, \quad k_B T_b = m_1 v_s^2. \quad (32)$$

All other parameters are the same as in Eq. (27).

The main goal is to investigate how fast the temperatures T_{11}, T_{22} of sublattices (FPUT particles and oscillators) become equal and how the maximum difference of the temperatures depends on the anharmonic parameter $\tilde{\beta}$ and the mass ratio γ .

A. Heavy oscillators ($\gamma = 2$)

We start with the weakly anharmonic case. The amplitudes of the kinetic temperatures, corresponding to $\gamma = 2$ and small anharmonic parameter $\tilde{\beta}$, are presented in Fig. 7. The figure shows that the heat transport preserves qualitative

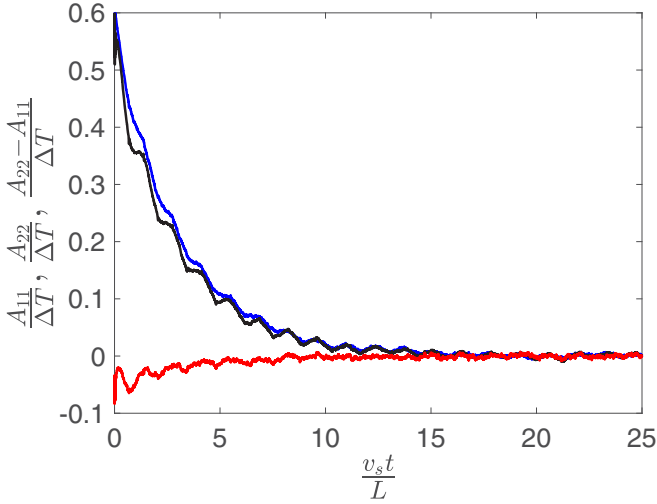


FIG. 8. The amplitudes A_{11} (blue line) and A_{22} (black line) of sinusoidal temperature profiles and their difference (red line) in case of strong anharmonicity ($\tilde{\beta} = 2$) for $\gamma = 2$.

features of the ballistic regime: oscillatory decay and significant difference between the temperatures of sublattices. The main effect of nonlinearity is that both amplitudes decay faster than in the harmonic case. However, the influence of nonlinearity on the temperature of the FPUT particles (A_{11}) is more significant than on the temperature of the oscillators (A_{22}). The behavior of A_{22} is described by the harmonic approximation [Eq. (26)] for times at least up to $v_s t/L \sim 10$ with reasonable accuracy. In contrast, the behavior of A_{11} coincides with the prediction of harmonic theory at much shorter times $v_s t/L \sim 1$. In the Sec. III D 3, it is shown that, in the harmonic case, acoustic vibrations give the main contribution to evolution of A_{11} (see Fig. 4), while optical vibrations mostly influence A_{22} . Then the influence of weak anharmonicity on acoustic vibrations is more significant than on the optical vibrations.

As expected, increasing the value of the anharmonic coefficient $\tilde{\beta}$ leads to transition from quasiballistic to diffusive⁴ regime of heat transfer (see Fig. 8). In the former case, the temperature performs decaying oscillations such that the amplitude changes sign [see Fig. 7(A)], while in the latter case the decay is monotonic. Our numerical simulations show that the value of $\tilde{\beta}$ of about 2 is sufficient to suppress the ballistic features of heat transfer for the considered chain length.⁵ For this value of $\tilde{\beta}$, the decay of amplitudes is almost monotonic. The difference between temperatures $A_{22} - A_{11}$ is smaller than A_{11} and A_{22} .

Thus in the case of heavy oscillators, the temperatures of sublattices are generally different. The difference between

⁴We suspect that the diffusion is anomalous and described by the fractional differential equation [53]. However, this question is beyond the scope of the present paper.

⁵In Ref. [52], it is shown that the value of nonlinearity coefficient β required for transition from ballistic to diffusive regime of heat transfer significantly depends on the wavelength of sine (number of particles). It decreases with increasing number of particles approximately as $1/\sqrt{N}$.

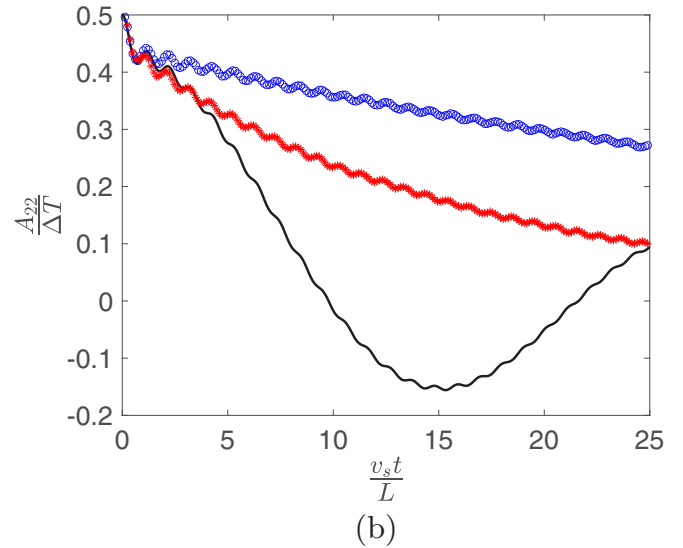
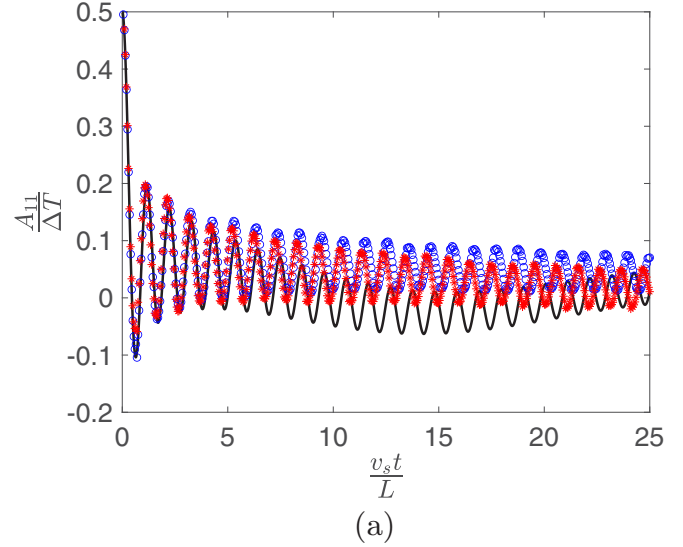


FIG. 9. The amplitudes A_{11} (a) and A_{22} (b) of sinusoidal temperature profiles in the weakly anharmonic case for $\gamma = 1/10$. The analytical solution [Eq. (26), solid line] and numerical simulation results for $\tilde{\beta} = 0.05$ (blue circles), $\tilde{\beta} = 0.1$ (red asterisks) are shown.

temperatures decreases with increasing nonlinearity coefficient (for further discussion see Sec. IV C).

B. Light oscillators ($\gamma = 1/10$)

As in the previous subsection, we start with the weakly anharmonic case. The amplitudes of the kinetic temperatures, corresponding to $\gamma = 1/10$ and small $\tilde{\beta}$, are presented in Fig. 9. It is seen from Fig. 9 that the influence of small nonlinearity is qualitatively similar to the previous case $\gamma = 2$. The decay of amplitudes remains oscillatory and its rate increases with increasing the nonlinearity coefficient. However, the influence of nonlinearity on the amplitudes A_{11} and A_{22} is exactly opposite: the influence on temperatures of the FPUT particles (A_{11}) is weak, while the influence on temperatures of the oscillators (A_{22}) is strong. Since the main contributions to A_{11} and A_{22} are given by acoustic and optical vibrations

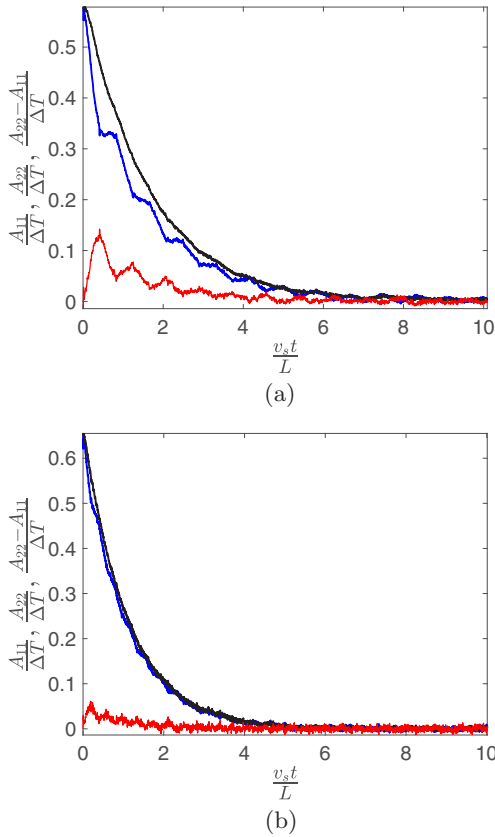


FIG. 10. The amplitudes A_{11} (blue line) and A_{22} (black line) of sinusoidal temperature profiles and their difference (red line) in the case of strong anharmonicity [$\tilde{\beta} = 2$ (a), $\tilde{\beta} = 100$ (b)] for $\gamma = 1/10$.

respectively [see Eq. (31)], then the influence of nonlinearity on optical vibrations is stronger (in contrast to the previous case).

As in the previous case ($\gamma = 2$), increase of the nonlinearity coefficient leads to transition from quasiballistic to diffusive regime of heat transfer. However, though for $\tilde{\beta} = 2$ the oscillations of temperatures are rather small and the decay is almost monotonic, this value is not sufficient for equalization and the temperatures remain significantly different during the heat transport [see Fig. 10(a)]. Our simulations show that equalization of temperatures requires significantly larger values of the anharmonic parameter $\tilde{\beta}$. Even for utterly strong anharmonicity ($\tilde{\beta} = 100$) there is still some finite difference of temperatures (amplitudes) [see Fig. 10(b)].

C. The maximum difference of temperatures

Simulation results, presented in Figs. 7–10, show that for both values of the mass ratio and all considered values of the nonlinearity coefficient there is some finite difference between the temperatures during the heat transfer. At the same time, the difference decreases with increasing nonlinearity coefficient. To demonstrate this decay, we plot the maximum difference between the temperatures $A_{22}-A_{11}$ for different values of $\tilde{\beta}$ and $\gamma = 2$ (see Fig. 11).

The figure shows that though the maximum difference is always finite, it practically may be neglected starting from

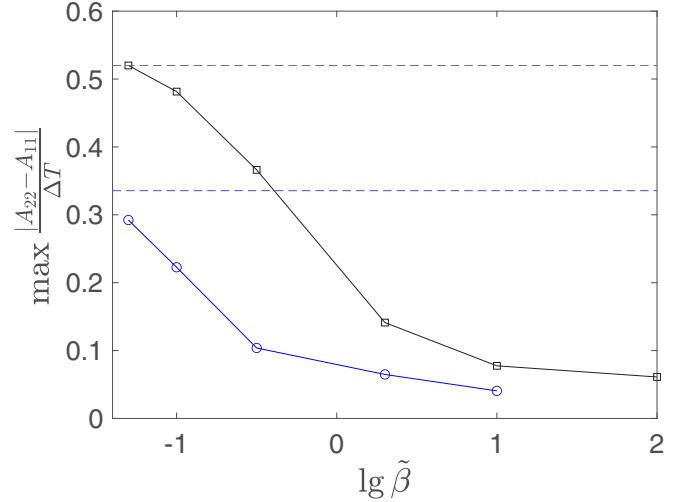


FIG. 11. Dependence of the maximum difference of temperatures on the nonlinearity coefficient for $\gamma = 2$ (blue circles) and $\gamma = 0.1$ (black squares). Dashed horizontal lines correspond to maximum difference in the harmonic case $\tilde{\beta} = 0$.

some “threshold” value of the nonlinearity coefficient. The specific choice of this threshold value is arbitrary and depends on the problem. It can be determined, for example, by the accuracy of temperature measurement or by what temperature difference in this particular problem should be considered as significant.

V. CONCLUSIONS

Features of unsteady heat transport in mass-in-mass chains were investigated. The main focus was on evolution of the two temperatures of sublattices (FPUT particles and oscillators) at different mass ratios and magnitudes of the nonlinearity.

In harmonic approximation, an analytical solution in form of integrals describing the evolution of an initial temperature profile was obtained. The solution allows to investigate and compare contributions of acoustic and optical vibrations to the heat transfer. It also shows that the temperatures of sublattices are equal initially and finally (at large times), while during the heat transfer they are significantly different. For small mass ratios, the closed-form solution for sinusoidal initial temperature profile was obtained. The solution shows that the temperatures of sublattices perform decaying oscillations with two significantly different main frequencies. The higher frequency of temperature oscillations is due to contribution of (low-frequency) acoustic vibrations of the chain, while the lower frequency is due to (high-frequency) optical vibrations of the chain. This new phenomenon is referred to as the ballistic spectra inversion.

In weakly anharmonic case, the characteristic features of ballistic heat transfer are also present. In particular, the temperatures remain significantly different. The anharmonic effects leads to faster decay of the temperature oscillations. This result is in a qualitative agreement with results for α -FPUT [40], β -FPUT [48,52], and ϕ^4 [49] chains. It was also shown that for mass ratios of order of unity ($\gamma \sim 1$), the nonlinearity mostly influences the temperature of the FPUT

particles, while the temperature of the attached oscillators remain almost unaffected. If the mass ratio is small ($\gamma \ll 1$), then the situation is exactly opposite.

Increase of the nonlinearity coefficient $\tilde{\beta}$ leads to the transition from the quasiballistic to diffusive regime of heat transfer (decay of sinusoidal temperature profile becomes almost monotonic). The maximum difference between the temperatures also decreases. However, even in the diffusive regime the temperature difference remains finite. Practically, the difference can be neglected starting from some threshold value of the nonlinearity coefficient. This threshold value increases with decreasing mass ratio γ .

We assume that the influence of nonlinearity on equalization of the temperatures can be interpreted in terms of timescales of different processes occurring in the heat conducting chain. The timescale of ballistic heat transport is proportional to the chain length divided by the average group velocity. The timescale of equalization of temperatures depends on the nonlinearity parameter $\tilde{\beta}$. For small $\tilde{\beta}$, this anharmonic timescale is much larger than the ballistic timescale and therefore the temperatures are different during the heat transfer. The anharmonic timescale decreases with increasing $\tilde{\beta}$ and the process of temperature equalization becomes faster. Therefore, starting from some threshold value of $\tilde{\beta}$ the temperatures equalize faster than they change due to heat transport. Derivation of estimates for the anharmonic timescale, determining the equalization, would be an important extension of the present work. We believe that these estimates can be obtained using the kinetic theory (see, e.g., Refs. [53–56]). In particular, the kinetic description of heat transfer in the β -FPUT chain is presented, e.g., in Ref. [53]. For the MiM chain this analysis could be extended by taking into account the optical quasiparticles. An important step in this direction has been taken in a recent paper [57], where a system of two coupled kinetic equations for acoustic and optical quasiparticles in the diatomic α -FPUT chain was derived. However, the behavior of the temperatures of two sublattices was not analyzed. We believe that further development of kinetic description of diatomic anharmonic chains will improve our understanding of equalization of the temperatures.

Presented results suggest that several distinct temperatures may be observed in heat conducting lattices consisting of

atoms of significantly different mass, e.g., in hydrocarbons ($\gamma = 1/12$). However, this theoretical prediction is awaiting for confirmation by molecular dynamics simulation of more realistic systems or by real experiments.

Our results may serve for the development of multicomponent continuum models with several temperatures, which are used, for example, for simulation of heat transfer in systems subjected to laser excitation (see, e.g., Refs. [10–13]). In these models, the behavior of the temperatures is governed by a coupled system of heat transfer equations, where the coupling is caused by energy exchange among the components. Results of our simulations may be used, e.g., for calibration and validation of the expressions, describing the coupling.

Finally, we note that presented results are closely related to the fundamental problem of defining the temperature (or temperatures) for systems far from equilibrium. In the literature, many definitions, including kinetic temperature, potential temperature, configurational temperature, etc., are introduced [14–16,58,59]. These definitions usually lead to identical results at equilibrium and differ in nonequilibrium cases. In the present paper, we used the kinetic temperature, because it has simple physical meaning and it can, in principle, be measured in real experiments. We also mention theoretical arguments in favor of the kinetic temperature, based on the possibility of constructing the ideal gas thermometer [59]. However, we note that the choice of proper definition for nonequilibrium temperature is an open problem and requires a separate study. We refer to review Refs. [14–16] for detailed discussion of this important problem.

ACKNOWLEDGMENTS

The work was supported by the Russian Science Foundation (Grant No. 21-71-10129). Simulations have been carried out using facilities of the Peter the Great Saint Petersburg Polytechnic University Supercomputing Center. The authors are deeply grateful to W. G. Hoover, D. A. Indeitsev, A. M. Krivtsov, A. V. Porubov, and S. A. Shcherbinin for useful and stimulating discussions. Valuable comments of the reviewers are highly appreciated.

-
- [1] R. Exartier and L. Peliti, A simple system with two temperatures, *Phys. Lett. A* **261**, 94 (1999).
 - [2] J. Fort, T. Pujol, and A. S. Cukowski, Several-temperature systems: Extended irreversible thermodynamics and thermal wavefront propagation, *J. Phys. A: Math. Gen.* **33**, 6953 (2000).
 - [3] B. L. Holian, W. G. Hoover, B. Moran, and G. K. Straub, Shock-wave structure via nonequilibrium molecular dynamics and Navier-Stokes continuum mechanics, *Phys. Rev. A* **22**, 2798 (1980).
 - [4] W. G. Hoover, C. G. Hoover, and K. P. Travis, Shock-Wave Compression and Joule-Thomson Expansion, *Phys. Rev. Lett.* **112**, 144504 (2014).
 - [5] S. I. Anisimov, V. V. Zhakhovskii, and V. E. Fortov, Shock wave structure in simple liquids, *JETP Lett.* **65**, 755 (1997).
 - [6] V. V. Zhakhovskii, K. Nishihara, and S. I. Anisimov, Shock wave structure in dense gases, *JETP Lett.* **66**, 99 (1997).
 - [7] A. Torrente, M. A. López-Castaño, A. Lasanta, Francisco Vega Reyes, A. Prados, and A. Santos, Large Mpemba-like effect in a gas of inelastic rough hard spheres, *Phys. Rev. E* **99**, 060901(R) (2019).
 - [8] N. A. Inogamov, Y. V. Petrov, V. V. Zhakhovsky, V. A. Hokhlov *et al.*, Two-temperature thermodynamic and kinetic properties of transition metals irradiated by femtosecond lasers, AIP Conf. Proc. No. 1464 (AIP, Melville, N.Y., 2012).
 - [9] D. A. Indeitsev and E. V. Osipova, A two-temperature model of optical excitation of acoustic waves in conductors, *Dokl. Phys.* **62**, 136 (2017).
 - [10] S. L. Sobolev, Two-temperature discrete model for nonlocal heat conduction, *J. Phys. III France* **3**, 2261 (1993).

- [11] S. L. Sobolev, Nonlocal two-temperature model: Application to heat transport in metals irradiated by ultrashort laser pulses, *Int. J. Heat Mass Transf.* **94**, 138 (2016).
- [12] A. Sellitto, I. Carlucci, and M. Di Domenico, Nonlocal and nonlinear effects in hyperbolic heat transfer in a two-temperature model, *Z. Angew. Math. Phys.* **72**, 7 (2021).
- [13] A. Bora, W. Dai, J. P. Wilson, and J. C. Boyd, Neural network method for solving parabolic two-temperature microscale heat conduction in double-layered thin films exposed to ultrashort-pulsed lasers, *Int. J. Heat Mass Transf.* **178**, 121616 (2021).
- [14] J. Casas-Vázquez and D. Jou, Temperature in nonequilibrium states: A review of open problems and current proposals, *Rep. Prog. Phys.* **66**, 1937 (2003).
- [15] J. G. Powles, G. Rickayzen, and D. M. Heyes, Temperatures: Old, new, and middle aged, *Mol. Phys.* **103**, 1361 (2005).
- [16] A. Puglisi, A. Sarracino, and A. Vulpiani, Temperature in and out of equilibrium: A review of concepts, tools and attempts, *Phys. Rep.* **709-710**, 1 (2017).
- [17] S. Lepri, R. Livi, and A. Politi, Thermal conduction in classical low-dimensional lattices, *Phys. Rep.* **377**, 1 (2003).
- [18] V. Kannan, A. Dhar, and J. L. Lebowitz, Nonequilibrium stationary state of a harmonic crystal with alternating masses, *Phys. Rev. E* **85**, 041118 (2012).
- [19] A. Kato and D. Jou, Breaking of equipartition in one-dimensional heat-conducting systems, *Phys. Rev. E* **64**, 052201 (2001).
- [20] T. N. Shah and P. N. Gajjar, Size dependent heat conduction in one-dimensional diatomic lattices, *Commun. Theor. Phys.* **65**, 517 (2016).
- [21] V. A. Kuzkin and A. M. Krivtsov, An analytical description of transient thermal processes in harmonic crystals, *Phys. Solid State* **59**, 1051 (2017).
- [22] V. A. Kuzkin and S. D. Liazhkov, Equilibration of kinetic temperatures in face-centered cubic lattices, *Phys. Rev. E* **102**, 042219 (2020).
- [23] V. A. Kuzkin, Unsteady ballistic heat transport in harmonic crystals with polyatomic unit cell, *Continuum Mech. Thermodyn.* **31**, 1573 (2019).
- [24] N. Boechler, J. K. Eliason, A. Kumar, A. A. Maznev, K. A. Nelson, and N. Fang, Interaction of a Contact Resonance of Microspheres with Surface Acoustic Waves, *Phys. Rev. Lett.* **111**, 036103 (2013).
- [25] L. Bonanomi, G. Theocharis, and C. Darai, Wave propagation in granular chains with local resonances, *Phys. Rev. E* **91**, 033208 (2015).
- [26] S. P. Wallen, J. Lee, D. Mei, C. Chong, P. G. Kevrekidis, and N. Boechler, Discrete breathers in a mass-in-mass chain with Hertzian local resonators, *Phys. Rev. E* **95**, 022904 (2017).
- [27] T. E. Faver, Small mass nanopteron traveling waves in mass-in-mass lattices with cubic FPUT potential, *J. Dynam. Diff. Eq.* **33**, 1711 (2021).
- [28] T. E. Faver, R. H. Goodman, J. Douglas Wright, Solitary waves in mass-in-mass lattices, *Z. Angew. Math. Phys.* **71**, 197 (2020).
- [29] H. H. Huang, C. T. Sun, and G. L. Huang, On the negative effective mass density in acoustic metamaterials, *Int. J. Eng. Sci.* **47**, 610 (2009).
- [30] G. L. Huang and C. T. Sun, Band gaps in a multiresonator acoustic metamaterial, *J. Vib. Acoust.* **132**, 031003 (2010).
- [31] V. I. Erofeev, D. A. Kolesov, and V. L. Krupenin, Dispersion and attenuation of a longitudinal wave propagating in a metamaterial defined as a mass-to-mass chain, *PNRPU Mechanics Bulletin*, No. 4 (2019), pp. 6–18 (in Russian), doi: 10.15593/perm.mech/2019.4.01.
- [32] A. V. Porubov and E. F. Grekova, On nonlinear modeling of an acoustic metamaterial, *Mech. Res. Commun.* **103**, 103464 (2020).
- [33] A. V. Porubov and I. D. Antonov, On control of harmonic waves in an acoustic metamaterial, *Mech. Res. Commun.* **116**, 103745 (2021).
- [34] A. V. Porubov, Wave modulation in a nonlinear acoustic metamaterial, *Int. J. Non Linear Mech.* **137**, 103788 (2021).
- [35] Xiaodong Cao, Dahai He, Hong Zhao, and Bambi Hu, Thermal expansion and its impacts on thermal transport in the FPU- α - β model, *AIP Adv.* **5**, 053203 (2015).
- [36] A. M. Krivtsov, Heat transfer in infinite harmonic one dimensional crystals, *Dokl. Phys.* **60**, 407 (2015).
- [37] V. A. Kuzkin and A. M. Krivtsov, Unsteady ballistic heat transport: Linking lattice dynamics and kinetic theory, *Acta Mech.* **232**, 1983 (2021).
- [38] V. A. Kuzkin and A. M. Krivtsov, Fast and slow thermal processes in harmonic scalar lattices, *J. Phys.: Condens. Matter* **29**, 505401 (2017).
- [39] A. Y. Panchenko, V. A. Kuzkin, and I. E. Berinskii, Unsteady ballistic heat transport in two-dimensional harmonic graphene lattice, *J. Phys.: Condens. Matter* **34**, 165402 (2022).
- [40] V. A. Kuzkin and A. M. Krivtsov, Ballistic resonance and thermalization in Fermi-Pasta-Ulam-Tsingou chain at finite temperature, *Phys. Rev. E* **101**, 042209 (2020).
- [41] M. B. Babenkov, A. M. Krivtsov, and D. V. Tsvetkov, Heat propagation in the one-dimensional harmonic crystal on an elastic foundation, *Phys. Mesomech.* **23**, 109 (2019).
- [42] M. B. Babenkov, A. M. Krivtsov, and D. V. Tsvetkov, Energy oscillations in a one-dimensional harmonic crystal on an elastic substrate, *Phys. Mesomech.* **19**, 282 (2016).
- [43] I. E. Berinskii and V. A. Kuzkin, Equilibration of energies in a two-dimensional harmonic graphene lattice, *Phil. Trans. R. Soc. A.* **378**, 20190114 (2020).
- [44] V. A. Kuzkin, Thermal equilibration in infinite harmonic crystals, *Continuum Mech. Thermodyn.* **31**, 1401 (2019).
- [45] I. Gelfand and G. Shilov, *Generalized Functions. Properties and Operations*, Vol. 1 (Academic Press, New York, 1964).
- [46] S. Huberman, R. A. Duncan, K. Chen, B. Song, V. Chiloyan, Z. Ding, A. Maznev, G. Chen, and K. Nelson, Observation of second sound in graphite at temperatures above 100 K, *Science* **364**, 6438 (2019).
- [47] Zhiwei Ding, Ke Chen, Bai Song, Jungwoo Shin, A. Maznev, K. Nelson, and G. Chen, Observation of second sound in graphite over 200 K, *Nat. Commun.* **13**, 285 (2022).
- [48] O. V. Gendelman and A. V. Savin, Nonstationary heat conduction in one-dimensional chains with conserved momentum, *Phys. Rev. E* **81**, 020103(R) (2010).
- [49] O. V. Gendelman, R. Shvartsman, B. Madar, and A. V. Savin, Nonstationary heat conduction in one-dimensional models with substrate potential, *Phys. Rev. E* **85**, 011105 (2012).
- [50] J. Candy and W. Rozmus, A symplectic integration algorithm for separable Hamiltonian functions, *J. Comput. Phys.* **92**, 230 (1991).
- [51] R. I. McLachlan and P. Atela, The accuracy of symplectic integrators, *Nonlinearity* **5**, 541 (1992).

- [52] E. A. Korznikova, V. A. Kuzkin, A. M. Krivtsov, Daxing Xiong, V. A. Gani, A. A. Kudreyko, and S. V. Dmitriev, Equilibration of sinusoidal modulation of temperature in linear and nonlinear chains, *Phys. Rev. E* **102**, 062148 (2020).
- [53] A. Mellet and S. Merino-Aceituno, Anomalous energy transport in FPU- β chain, *J. Stat Phys.* **160**, 583 (2015).
- [54] H. Spohn, The Phonon Boltzmann Equation, properties and link to weakly anharmonic lattice dynamics, *J. Stat Phys.* **124**, 1041 (2006).
- [55] M. Onorato, L. Vozella, D. Proment, and Y. Lvov, Route to thermalization in the α -Fermi-Pasta-Ulam system, *Proc. Natl. Acad. Sci. USA* **112**, 4208 (2015).
- [56] Y. Lvov and M. Onorato, Double Scaling in the Relaxation Time in the β -Fermi-Pasta-Ulam-Tsingou Model, *Phys. Rev. Lett.* **120**, 144301 (2018).
- [57] A. Pezzi, G. Deng, Y. Lvov, M. Lorenzo, and M. Onorato, Three-wave resonant interactions in the diatomic chain with cubic anharmonic potential: Theory and simulations. [arXiv:2103.08336](https://arxiv.org/abs/2103.08336).
- [58] T. Hatano and D. Jou, Measuring temperature of forced oscillators, *Phys. Rev. E* **67**, 026121 (2003).
- [59] W. G. Hoover, B. L. Holian, and H. A. Posch, Comment I on Possible experiment to check the reality of a nonequilibrium temperature, *Phys. Rev. E* **48**, 3196 (1993).